Journal of Pain Research

Dovepress
Taylor & Francis Group

Open Access Full Text Article

METHOD

Establishing an Electrophysiological Recording Platform for Epidural Spinal Cord Stimulation in Neuropathic Pain Rats

Chin-Tsang Yang[1–3], Bai-Chuang Shyu[1], Wei-Tso Lin[4], Kuo-Hsiang Lu[4], Chung-Ren Lin[5], Yeong-Ray Wen[6–8,*], Chih-Cheng Chen[1,9,10,*]

[1]Institute of Biomedical Sciences, Academia Sinica, Taipei, Taiwan; [2]Department of Leisure Industry and Health Promotion, National Ilan University, Yilan, Taiwan; [3]Department of Biotechnology and Animal Sciences, National Ilan University, Yilan, Taiwan; [4]Gimer Medical Co., New Taipei City, Taiwan; [5]Department of Anesthesiology, National Cheng Kung University Hospital, Tainan, Taiwan; [6]Pain Management and Research Center, Department of Anesthesiology, China Medical University Hospital, Taichung, Taiwan; [7]Chun Chuan Orthopedic and Pain Specialty Hospital, Taichung, Taiwan; [8]Pain Management Center, Department of Anesthesiology, Jen-Ai General Hospital, Taichung, Taiwan; [9]Neuroscience Program of Academia Sinica, Academia Sinica, Taipei, Taiwan; [10]Taiwan Mouse Clinic, Biomedical Translational Research Center, Academia Sinica, Taipei, Taiwan

*These authors contributed equally to this work

Correspondence: Chih-Cheng Chen; Yeong-Ray Wen, Email chih@ibms.sinica.edu.tw; yray.wen@gmail.com

Purpose: Spinal cord stimulation (SCS) is pivotal in treating chronic intractable pain. To elucidate the mechanism of action among conventional and current novel types of SCSs, a stable and reliable electrophysiology model in the consensus animals to mimic human SCS treatment is essential. We have recently developed a new in vivo implantable pulsed-ultrahigh-frequency (pUHF) SCS platform for conducting behavioral and electrophysiological studies in rats. However, some technical details were not fully understood. This study comprehensively analyzed methodology and technical challenges and pitfalls encountered during the development and implementation of this model.

Materials and Methods: Employing a newly developed pUHF-SCS (±3 V, 2 Hz pulses with 500-kHz biphasic radiofrequency sinewaves), we assessed analgesic effect and changes of evoked local field potentials (eLFPs) in the bilateral primary somatosensory and anterior cingulate cortices in the rats with or without spared nerve injury (SNI) using the platform. The placement of stimulating needle electrodes in the hind paw was examined and optimized for functionality.

Results: SNI enhanced the C component of eLFPs in bilateral cortexes elicited by stimulating the contralateral but not the ipsilateral lateral aspect of the hind paw. Repeated pUHF-SCS significantly reversed SNI-induced paw hypersensitivity and reduced C-component enhancement. An impedance test can determine an optimal SCS electrode function: an SCS discharge threshold of 100–400 μA for cortical activation or a motor threshold of 150–600 μA for the hind limbs. Impedance increased due to growth of fibrotic tissue but stabilized after post-implantation day 12.

Conclusion: We presented a reliable electrophysiological platform for SCS application in rat neuropathic pain model and demonstrated potent analgesic effects of pUHF-SCS. All device implantations or pUHF-SCS per se did not cause evident spinal cord damage. This safe and stable platform provides an in vivo rat model for SCS investigation of mechanisms of action and device innovation.

Keywords: spinal cord stimulation, pulsed-ultrahigh-frequency, evoked local field potential, primary somatosensory cortex, anterior cingulate cortex

Introduction

Neuropathic pain accounts for 15–25% of all chronic pain conditions.[1] However, pharmacotherapy alone provides insufficient pain relief. Spinal cord stimulation (SCS) has been used to treat chronic intractable neuropathic syndromes for a long time.[2] Conventional SCS was developed based on the gate control theory and uses a low-frequency (40–100 Hz) stimulation (LF-SCS) to generate the analgesic effect. Modern SCS paradigms, including high-frequency (10 kHz) SCS (HF-SCS), burst SCS, closed-loop SCS, differential target multiplexed SCS, and our invention, pulsed ultrahigh-frequency

Received: 4 August 2024
Accepted: 19 December 2024
Published: 21 January 2025

SCS (pUHF-SCS),[3,4] were developed in recent decades to overcome the limitations of unsatisfactory effectiveness and unpleasant paresthesia sensation of conventional LF-SCS.[2] These new types of SCS exhibit diverse stimulation parameters, in terms of electrical frequencies, stimulation mode, and delivered power, leading to high analgesic efficacy and improvements in affection/cognition aspect, and functionality. Additionally, studies have shown that these modern SCS paradigms could have distinct neurophysiological mechanisms of action (MoA).[5]

Although excellent SCS animal studies had been proposed,[6–8] there is no methodological consensus in mimicking human SCS treatment, and experimental obstacles including awakened animals, electrical parameters, long-term implantation, disproportionately large SCS lead to the rat's spinal cord, and brain responses, all become great challenges to animal studies. Two brain regions greatly contribute to chronic pain modulation. The primary somatosensory cortex (S1) is recognized for encoding the sensory-discriminative aspect of pain, while the anterior cingulate cortex (ACC) represents the affective-motivational dimension of pain.[9] The development of a reliable animal model and advanced brain recording techniques is essential to enhance our understanding of how various stimulation parameters (eg, amplitude, frequency, pulse width [PW], and waveform) affect the brain and to explore their distinct MoA.

This study was an extension of our previous article in *Anesthesiology* to address details in methodology and technical pitfalls in developing this implantable SCS animal model and an in vivo electrophysiological recording system.[3] A newly developed pUHF-SCS was utilized to evaluate the feasibility and functionality of the platform and to assess its analgesic effects.

Materials and Methods

Male Sprague–Dawley rats (350–450 g, sourced from BioLASCO, Taipei, Taiwan) were housed in an air-controlled environment (21°C–23°C, 50% humidity, 12/12-hour light/dark cycle with lights on at 08:00 am) with unrestricted access to food and water at Academia Sinica, Taiwan. All experiments were conducted following the standard ethical guidelines of the Academia Sinica Institutional Animal Care and Utilization Committee (IACUC) under the ethical protocol ID: 23–06-2018. After major surgeries, the rats were immediately given intraperitoneal antibiotic injections (50 mg/kg ceftriaxone in 250 μL saline; Sandoz GmbH, Kundl, Austria) to prevent postoperative infection and were allowed to recover for one week.

Behavioral Assessment

Mechanical hypersensitivity was assessed using von-Frey filaments (Stoelting, Wood Dale, IL, USA) with the up-down method to determine the 50% paw withdrawal threshold (PWT).[10] Rats were individually placed in a Plexiglas cage's chamber, and the lateral plantar surface of the hind paw was stimulated using one of the eight von-Frey fibers with incremental strength (0.4–26.0 g). The PWTs were determined daily for at least two days before SNI surgery (preoperative baseline) and at various time points before and after SCS. The investigator conducting the behavioral tests was blind to the treatment group.

SNI Model of Neuropathic Pain

The SNI surgery was performed as previously described.[11] Briefly, the tibial and common peroneal nerves in the left hind thigh of rats were ligated using a 5–0 silk suture, followed by transection and removal of a 2 mm nerve segment distal to the ligation. The sural nerve was carefully separated to ensure its integrity without over-stretching. The thigh muscles and skin were sutured, and the rats were returned to cages for recovery. In this model, neuropathic pain was assessed in the sural nerve territory. Additionally, those rats not exhibiting mechanical hypersensitivity, with a PWT >6 g at post-SNI 7–10 days, were excluded from the study.

The Rodent SCS Electrode and Epidural Implantation Surgery

The SCS device was manufactured by GIMER Medical Co. (New Taipei City, Taiwan). The featured bipolar stainless-steel electrode (diameter: 1.5 mm, center spacing: 2 mm) encased in medical-grade silicone was connected to two silver-core wires (35N LT) that passed through a wing anchor to link to a two-pin connector (gold-plated brass) for an external neurostimulator (Figure 1A). The rats were initially anesthetized with 3% isoflurane in oxygen and maintained with 1.5% isoflurane in oxygen during surgery. Body temperature of 36.5°C–37.5°C was maintained throughout the surgery using a homeothermic blanket

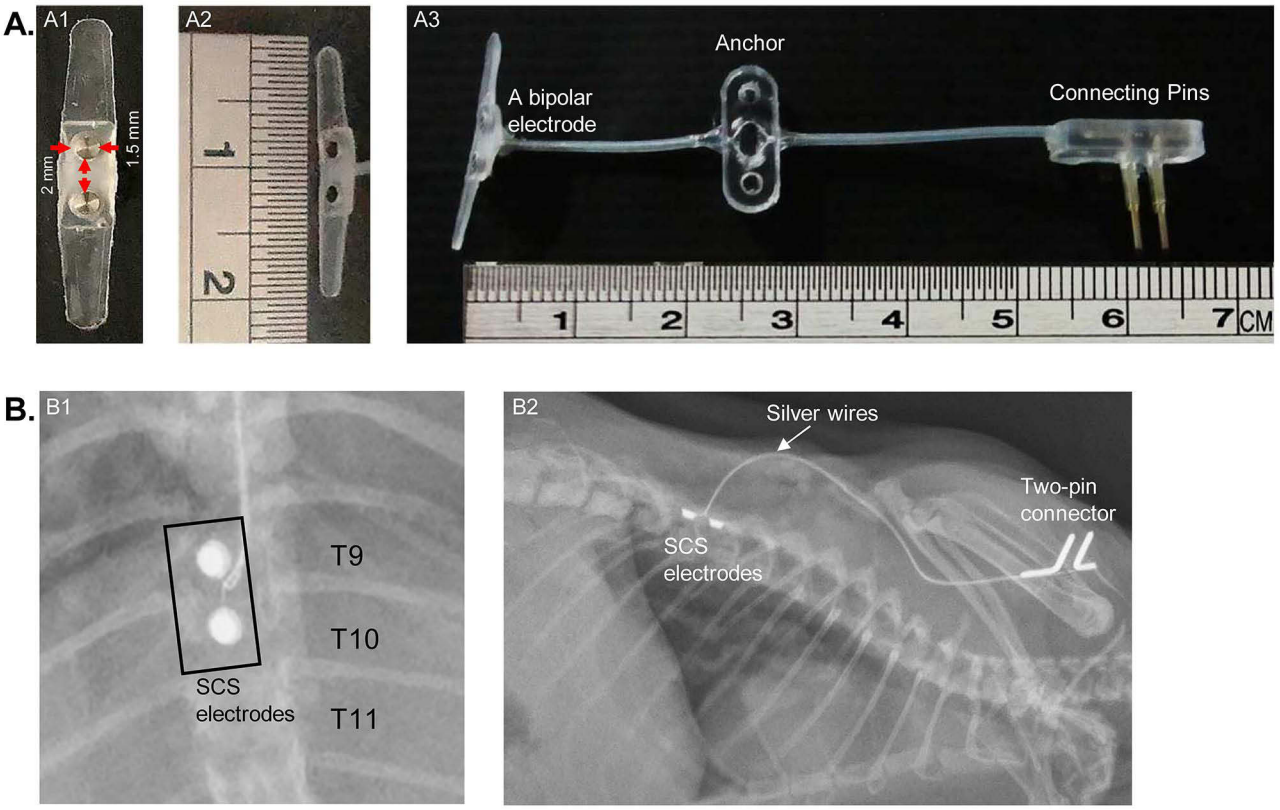

Figure 1 Photo and X-ray images illustrating the spinal cord stimulation electrode and implantation in a rat spinal cord. (**A**) Rodent SCS Device: (**A1**), (**A2**). Anterior-posterior and lateral views of a bipolar stainless-steel electrode (diameter: 1.5 mm, center spacing: 2 mm); (**A3**). A SCS device encased in medical-grade silicone, featuring a bipolar electrode connected with two silver-core wires passing through a wing anchor, and linked to a two-pin connector for an external neurostimulator. (**B**) X ray images of epidural SCS Device at thoracic T9–T11 Vertebrae: (**B1**), (**B2**). Posterior-anterior and lateral views of X-ray images depicting a rat implanted with an SCS device.

system (model 50–7079, Harvard Apparatus, Holliston, MA, USA), and the respiratory rate was continually monitored. A laminectomy was performed at the thoracic T9–T11 vertebrae to expose the spinal cord. The bipolar SCS electrode was carefully inserted into the spinal epidural space (Figure 2A1), which was confirmed by postoperative X ray images (Figure 1B). After hemostasis, the muscle and fascia were covered and sutured by layers with 4–0 silk (Figure 2A2). The wing anchor was secured onto the muscle (Figure 2A2), and silver-core wires were tunneled under the skin to the posterior nuchal area with two pins protruding for future external neurostimulator connection. The skin wound was closed with sutures (Figure 2A3). An antibiotic was sprayed over the surgical field during the surgery and was administered intraperitoneally before and daily for three days after surgery. Animals were granted a recovery period of 7–10 days post-surgery.

Implantation of Brain Recording Electrodes

For brain implantation, the rats were maintained anesthetized under 1.5% isoflurane throughout the surgery. Body temperature of 36.5°C–37.5°C and the respiratory rate were continuously monitored. After removing the scalp hair, a midline incision was made to expose the skull. Six craniotomy holes were performed for electrode implantation. The brain electrode utilized two parallel small stainless-steel screws threaded through holes in the skull. Two pairs of electrodes were placed onto the bilateral S1 of the hind limb (S1HL, 1.5 mm posterior and 2.5 mm lateral to the bregma) and the ACC (1.3 mm anterior and 0.5 mm lateral to the bregma) (Figure 2B1). Two additional small stainless-steel screws were anchored onto the skull, one serving as a reference electrode (+9 mm to the bregma) and the other as a grounding electrode (−12 mm to the bregma). All six electrodes were connected to an Omnetics 16-pin micro-connector, and the entire electrode assembly was insulated and secured onto the skull with dental acrylic. Finally, the wound was closed by layers, and the skin was sutured with 4–0 silk (Figure 2B1–B2).

https://doi.org/10.2147/JPR.S489420

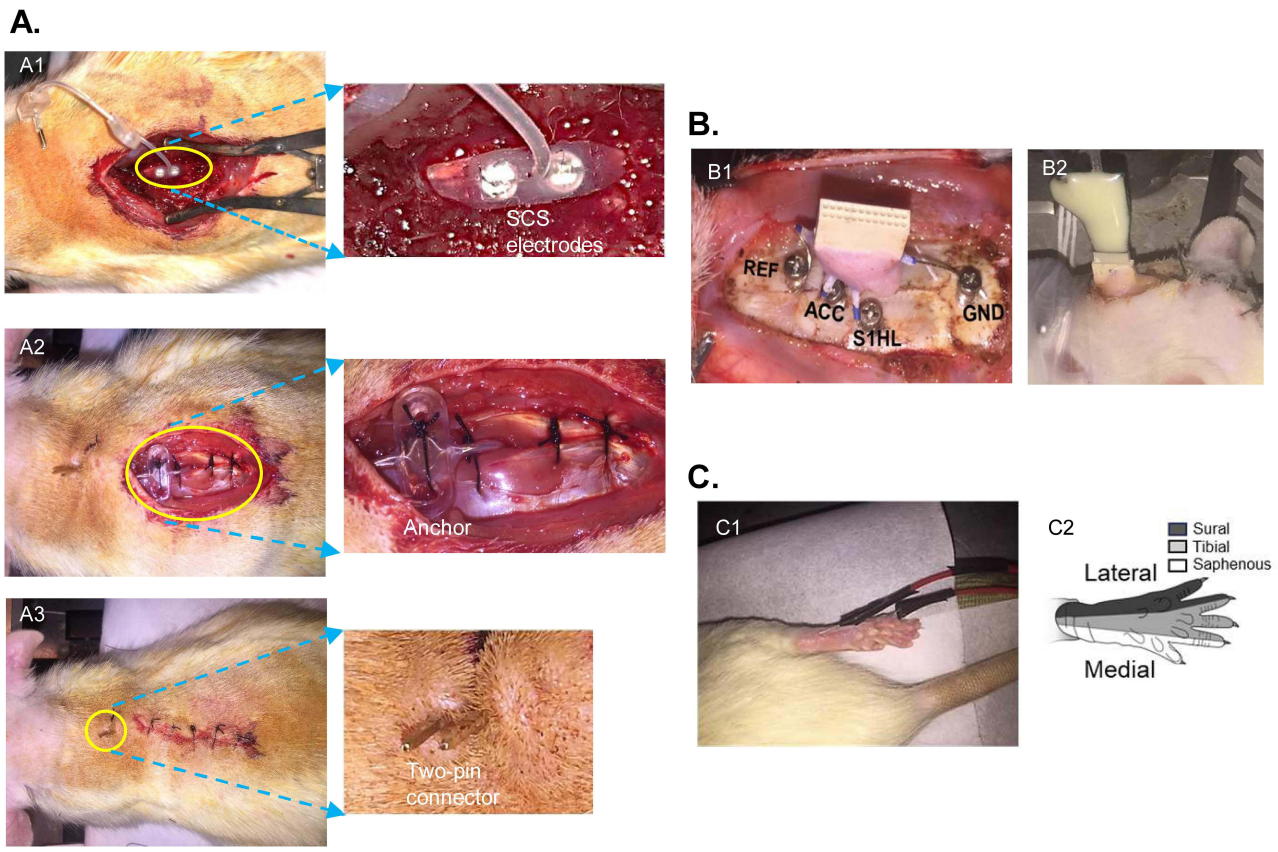

Figure 2 The illustration for surgical Implantation of the SCS and brain recording devices. (**A**) Photos of the steps for SCS implantation: (**A1**). A laminectomy on T9 to T11 and epidural placement of SCS electrodes; (**A2**). The electrodes were secured with muscle sutures, the anchor was attached to the muscles, and the electrode wires were subcutaneously tunneled to the posterior nuchal area; (**A3**). The wound was closed in layers, and the pins were left exposed through the skin to enable connection to an external neurostimulator. (**B**) Photos for brain electrode implantation: (**B1**). One pair of bilateral stainless-steel bunt screws, serving as brain electrodes, were anchored onto the surface of the primary somatosensory cortex of the hind limb (S1HL) and the anterior cingulate cortex (ACC), with another two screws as reference (REF) and ground electrodes (GND). The brain electrodes were connected to a 16-pin micro-connector insulated and bonded to the skull using dental acrylic. (**B2**). The entire brain electrode assembly was insulated and bonded to the skull with dental acrylic and covered by skin sutures for connections to the external recording system. (**C**) Photo of hind-paw electrical stimulation: (**C1**). Two stainless-steel needle electrodes (0.5 mm in diameter, positioned 1.2 cm apart) for electrical stimulation were subcutaneously inserted at the hind paw's lateral aspect between the hairy and glabrous skin over the fifth toe; (**C2**). Innervation mapping of the rat's hind paw.

Recording Evoked Local Field Potentials (eLFPs) of the S1HL and ACC Elicited by Electrical Stimulation at the Hind Paw

A pair of stainless-steel needle electrodes, each with a 0.5 mm diameter and positioned 1.2 cm apart, were subcutaneously inserted into the palmar surface at the hind paw's lateral border (Figure 2C). The electrical stimulation was administered through a pulse generator (model 2100; A-M Systems, Carlsborg, WA, USA) with the parameters of biphasic pulses, 1 ms PW at a frequency of 0.1 Hz, and amplitude of 0.5–10 mA.

Under stable anesthesia with 1.5% isoflurane, the eLFPs in the S1HL and ACC in response to hind paw electrical stimulation were recorded, amplified, and filtered (0.1–50 Hz) using a multichannel data acquisition system (TDT; Alachua, FL, USA) and monitored for 10–15 minutes until stabilization. The eLFPs recorded at the S1HL or ACC for 20 electrical stimuli were averaged and analyzed using MATLAB software (The MathWorks, Natick, MA, USA). The stability of eLFPs was achieved at 7–10 days after brain implantation and constantly examined for at least one month (data not shown).

Platform (Model) Setup and Study Design

This rat platform for SCS, SNI, peripheral electrical stimulation, and brain recording is illustrated in Figure 3A–B. pUHF-SCS was delivered by a GIMER medical neurostimulator (ES1001; New Taipei City, Taiwan) outputting a 2 Hz wave with a 25 ms pulse width (PW). Each pulse comprises a 500 kHz sine wave at an amplitude of ± 3.0 V (Figure 3C), based on our published studies.[3,12]

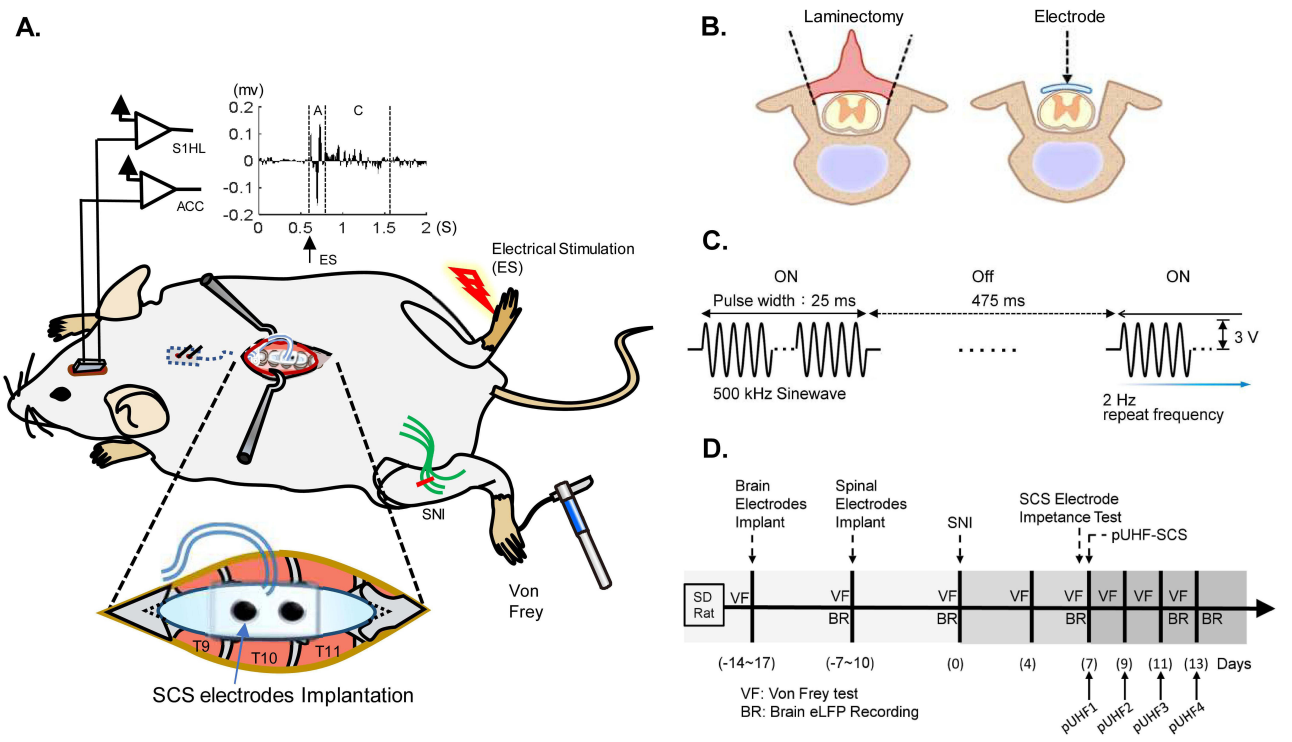

Figure 3 Illustration of an epidural implantable Spinal Cord Stimulation (SCS) platform for behavioral and electrophysiological studies in rats. (**A**) Overview of the rat model demonstrating SCS electrode implantation, brain recording device for eLFP at S1HL and ACC in response to electrical stimulation of the right hind paw contralateral to spared nerve injury (SNI), and von-Frey test for behavioral assessment. The schematic image is adapted from our previous submission;[3] (**B**) Surgical procedure of laminectomy for placement of SCS electrode on the spinal dura; (**C**) Representation of the wave pattern and stimulation parameters of pUHF-SCS; (**D**) Timeline outlining the study procedures.

The experimental design comprised three phases (Figure 3D): (1) the implantation of the cortical recording device and then the SCS device, (2) SNI surgery, and (3) pUHF-SCS. Each stage involved measuring body weight, conducting behavioral tests, recording brain activity, and checking electrode contact through impedance tests. The rats were allowed to recover for seven days after each surgery. In Phase 3, pUHF-SCS was administered three times every two days, and mechanical PWTs were measured before pUHF-SCS and at one hour, three hours, five hours, and one day after pUHF-SCS. Brain eLFPs were examined before and after the fourth pUHF-SCS treatment.

All rats were randomly assigned into three groups: SNI with sham pUHF-SCS (SNI+sham pUHF), SNI with repeated 20-minute pUHF-SCS (SNI+pUHF-20 m), and sham SNI with repeated 20-minute pUHF-SCS (sham SNI+pUHF-20 m). Individual experiments included rats from different groups to minimize biases. Considering the complexity of the three major surgeries, we had a six-month surgical practice period before the actual study[3] to standardize the procedures and to minimize surgery-related complications. Therefore, we could reduce the rat number to 22 in this study, with 17 successful completions and only 5 withdrawals (Table 1). Among the withdrawn rats, one developed a local infection, one exhibited

Table 1 Number of Experimental Animals

Group	Rat Completed the Study.	Excluded Num.					Total Excluded Num.	Total Num.
		Brain Electrode: Impedance Test Failed	Infection	Neurological Deficits	SCS Electrode: Impedance test failed	PWT >6 g		
SNI+pUHF-20 m	6	1	1		1		3	9
Sham SNI+pUHF-20 m	7			1			1	8
SNI+ Sham pUH-20 m	4					1	1	5
SUM	**17**						**5**	**22**

https://doi.org/10.2147/JPR.S489420

walking deficits/(neurological deficits) within seven days post-SCS implantation, one did not show mechanical hypersensitivity seven days post-SNI, and two did not pass the SCS and brain impedance test seven days post-implantation (Table 1).

Impedance Testing and Exclusion Criteria for Identifying Poor SCS Electrode Function

Despite the careful placement of the SCS device in surgery, potential complications may occur including electrode displacement or migration, device-induced spinal cord compression or injury, or infection. We developed an impedance test to validate the correct function of the SCS device and conducted the test at least once per week to ensure optimal current conductivity. The threshold for inducing cortical eLFPs by SCS charge (PW = 1 ms, 0.1 Hz, biphase) was determined by gradually increasing the SCS current amplitude from 0 to the minimum intensity that activated cortical action potentials. Another test is to detect motor threshold (MoT) by observing movement in the lower trunk or hind limbs as SCS intensity was gradually increased. The rats showing signs of infection (eg, wound rupture, discharge, or pus formation), neurological deficits (eg, limping, drop limb, or body distortion), or a high SCS threshold indicating high electric impedance (ie, a current threshold for 0.1 Hz SCS to evoke cortical eLFPs exceeding 600 μA or an MoT exceeding 800 μA and possible electrode displacement, migration, or wire detachment) were excluded from the study.

Pitfalls of Optimizing Needle Electrode Placement at the Hind Paws to Induce Maximal eLFP Responses in the SNI Rats

To capture the maximal eLFP responses, we made efforts to compare the cortical eLFPs evoked by different methods of needle electrode insertions at the hind paw. At the pre-study experimental period, we disappointedly obtained unstable and unpredictable brain recording data evoked by left or right hind paw stimulation; therefore, we conducted several trials to test optimal needle placement positions at different aspects of the right or left hind paw and the depth of the injection. Finally, we successfully identified and determined the precise positions through electrical stimulation of the contralateral hind paw, but not the ipsilateral hind paw, in SNI rats. These positions were used in subsequent experiments to evaluate whether SCS modulates the evoked brain potentials (Figures 4A and 2C). The rationale for this approach will be explained in the following Results and Discussion sections.

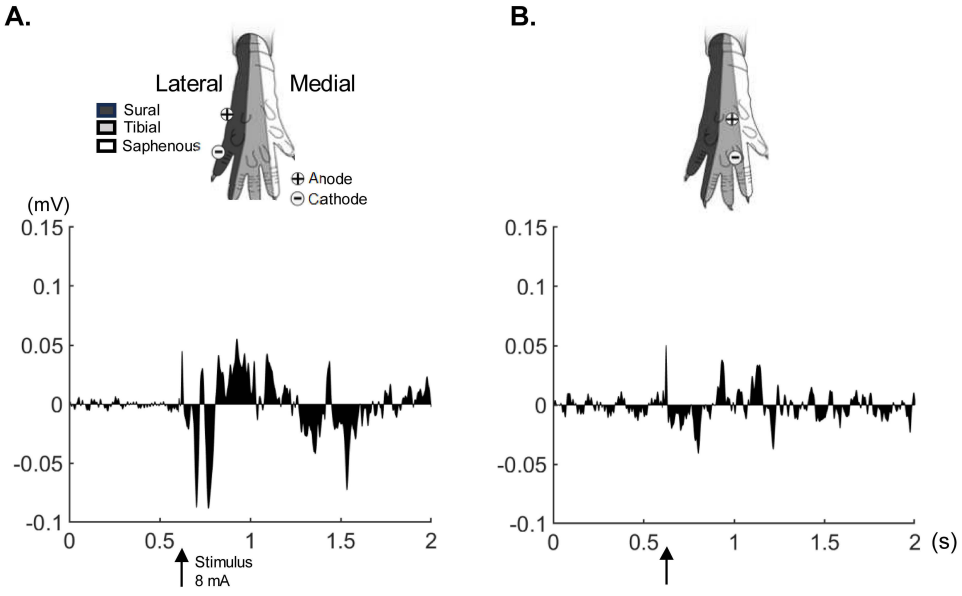

Figure 4 Comparison of cortical evoked local field potentials (eLFP) in rat with spared nerve injury (SNI) following hind paw electrical stimulation targeting the sural and tibial nerve territories. (**A**) Stainless-steel needle electrode insertion at the sural nerve territory to induce brain eLFP in the right primary somatosensory cortex of the hind limb (S1HL) on day 7 post-SNI. (**B**) eLFP response elicited by tibial nerve territory stimulation on day 7 post-SNI.

Statistical Analyses

Nociceptive thresholds were compared using a two-way repeated measures analysis of variance (RM-ANOVA). Brain eLFPs before and after SNI or SCS electrode implantation were compared using a paired *t*-test. The MoT and electrical threshold of cortical eLFPs were compared using a *t*-test. The impedance of the different high-frequency SCS electrodes was compared using one-way RM- ANOVA at the post-SCS time point. Post hoc analyses were conducted with Tukey's test for multiple comparisons when applicable. Data are presented as the mean ± standard error of the mean (SEM). A $p < 0.05$ was considered statistically significant. Statistical analyses were conducted using Prism 10.1.1 software (GraphPad Software Inc., San Diego, CA, USA).

Results

The Optimal Location for Stimulating Needle Electrodes at the Paw

After repetitive trials, we defined that the most effective configuration for brain recordings was the insertion of a pair of needle electrodes spaced 1.2 cm apart, 5 mm-length at subcutaneous tissue, and at the lateral border of the hind paw, positioned approximately between the hairy and glabrous skin over the fifth toe (Figures 4A and 2C). In comparison, a needle inserted in a length of 3 mm subcutaneously may be easily dislodged, while a length of 10 mm often caused ecchymosis compared with the length of 5 mm. Notably, electrical stimulation of the lateral paw (the sural nerve-innervated area, Figure 4A) produced greater cortical eLFPs at the S1HL than stimulation at the mid paw (the tibial nerve-innervated area, Figure 4B).

SNI Enhanced the C-Components of eLFPs Elicited by Electrical Stimulation at the Contralateral but Not the Ipsilateral Hind Paw

Without electrical stimulation at the hind paw, the eLFPs at the S1HL were quiescent with or without SNI (Figure 5A–B, left). However, 7–10 days post-SNI, eLFPs at the S1HL and ACC induced by 1 mA stimulation at the contralateral (or right) hind paw showed evident increases compared to its pre-SNI level (Figure 5A–B, right). We defined eLFP waveforms by two components based on the nerve conduction velocity: the A component (10–220 ms after electrical stimulation at the hind paw, including Aβ and Aδ fiber-mediated transmission) and the C component (220–1010 ms, C fiber-mediated transmission) (Figure 5A–B). The area under the curves (AUCs) of eLFPs showed a parallel stepwise increase with stimulation intensities from 0.5, 1.0, to 5.0 mA (Figure 5C and D) before SNI. After SNI, AUCs of the C component induced by 0.5 and 1 mA stimulations at the right hand paw were significantly higher than at the pre-SNI phase (Figure 5C, right), and similar increases were observed in the bilateral S1HL and ACC and indifferent between hemispheres. The lack of change in the C component with 5 mA stimulation could be due to the high-intensity stimulation obscuring the response differences (Figure 5C). Notably, AUCs of the A component did not change after SNI (Figure 5C, left). Unexpectedly, eLFPs at the post-SNI phase evoked by stimulation at the left hind paw (ie, ipsilateral to SNI) did not showed the same changes as those at the right hind paw due to high variations in the recordings (Figure 5D). Therefore, we applied electrical stimulation at the contralateral hind paw in the subsequent experiments.

Impedance Tests to Ensure Optimal SCS and Brain Electrode Function

An intact contact between the implanted SCS electrode and the spinal dura ensures the effective transmission of stimulating signals into the spinal cord. The threshold for cortical eLFPs elicited by SCS discharge with biphasic waves at a frequency of 0.1 Hz and pulse width of 1 ms ranging from 100 to 400 μA (Figure 6A and B). In our recently published study,[3] rats undergoing regular impedance tests with a current threshold within 100–400 μA showed positive outcomes of pUHF-SCS-induced analgesia. As a result, we designated a threshold below 400 μA as the optimal electrode contact with the spinal cord. The rats with an SCS current higher than 600 μA (Figure 6C), implicating a high electric impedance, were excluded from the study. We also found that brain electrodes in some rats developed high impedance; rats should be excluded from subsequent experiments whenever the eLFP amplitudes evoked by 1 mA hind paw stimulation decrease suddenly by more than 50%.

The MoT may serve as an additional indicator for the optimal SCS electrode function. We found that the MoT was, on average, 1.6-fold higher than the average threshold for inducing cortical eLFPs (Figure 6D). Therefore, a MoT of

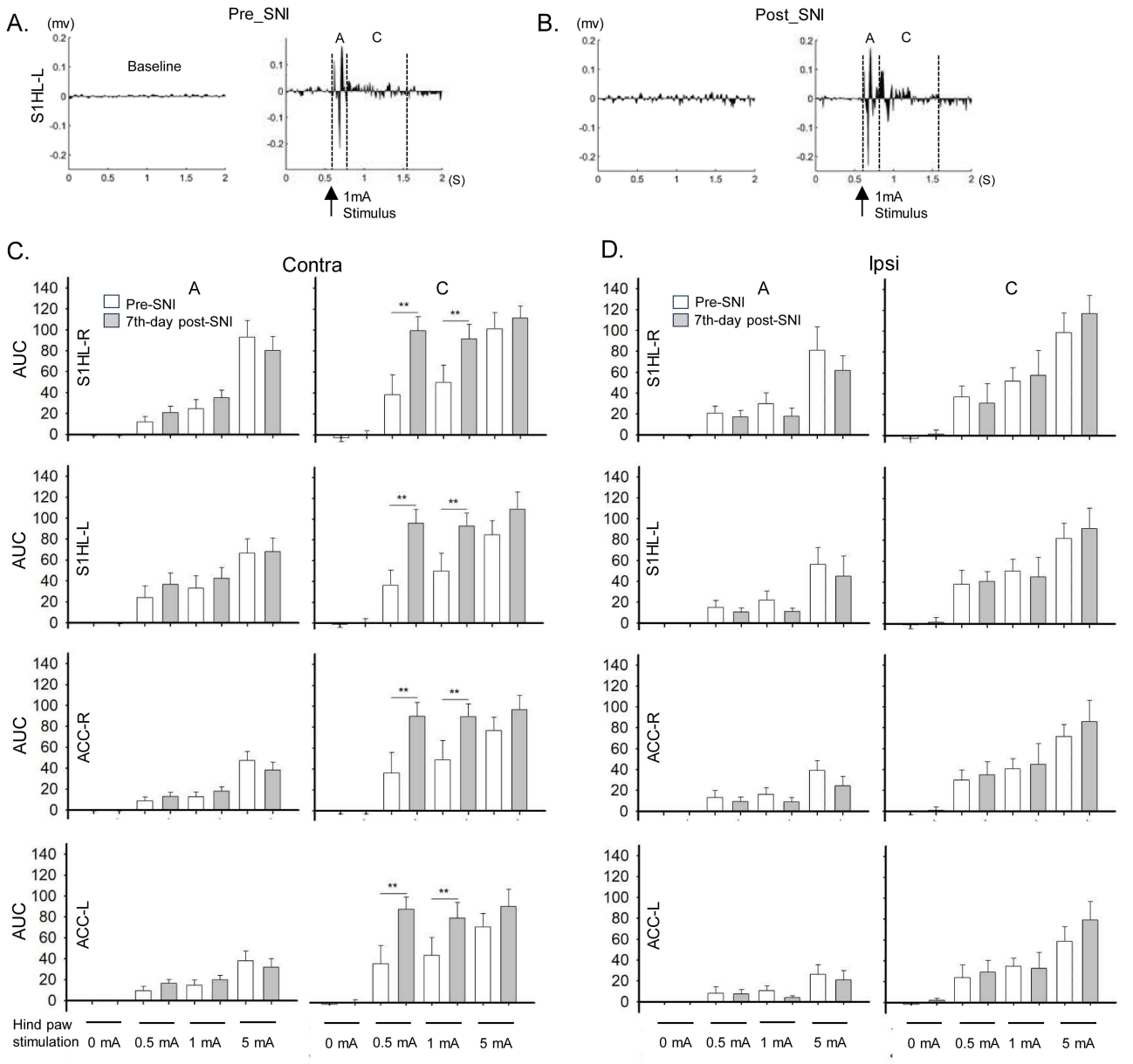

Figure 5 Comparisons of evoked local field potentials (eLFPs) elicited by hind paw stimulation in the primary somatosensory cortex of the hind limb (S1HL) and the anterior cingulate cortex (ACC) between the naïve and the spared nerve injury (SNI) rats. (**A**) Example of pre-SNI recordings of eLFPs at the left S1HL for baseline (no stimulation) and 1 mA paw stimulation. The 1 mA stimulation produced eLFPs with an A component (10–220 ms after stimulation, mediated by Aβ and Aδ fibers) and a C component (220–1010 ms after stimulation, mediated by C fibers). (**B**) Example of post-SNI recordings of eLFPs at the left S1HL for baseline (no stimulation) and 1 mA paw stimulation. (**C**) Area under the curves (AUC) of C-components and A-components of eLFPs in bilateral S1HL and ACCs elicited by stimulation at the hind paw contralateral (Contra.) to SNI. (**D**) AUCs of and C-components and A-components of eLFPs in bilateral S1HL and ACC elicited by stimulation at the hind paw ipsilateral to SNI. N = 8; ** $p < 0.01$ between groups; paired *t*-test.

150–600 μA represents an optimal electrode contact. The rats with a MoT of 150–600 μA showed effective pUHF-SCS-induced analgesia. Rats with MoT threshold exceeding 800 μA were excluded from the study.

pUHF-SCS Produced a Prolonged Inhibition of Mechanical Hypersensitivity and Attenuated Cortical Activations to Noxious Stimulation

We replicated our previous study,[3] utilizing a 20-minute pUHF-SCS, and reproduced similar inhibition of SNI-induced mechanical hypersensitivity. The PWTs of the nerve-injured hind paw decreased significantly from baseline (23–24 g) to <2 g post-SNI in all rats, which persisted for at least two weeks (Figures 7A, black line). The PWTs did not change

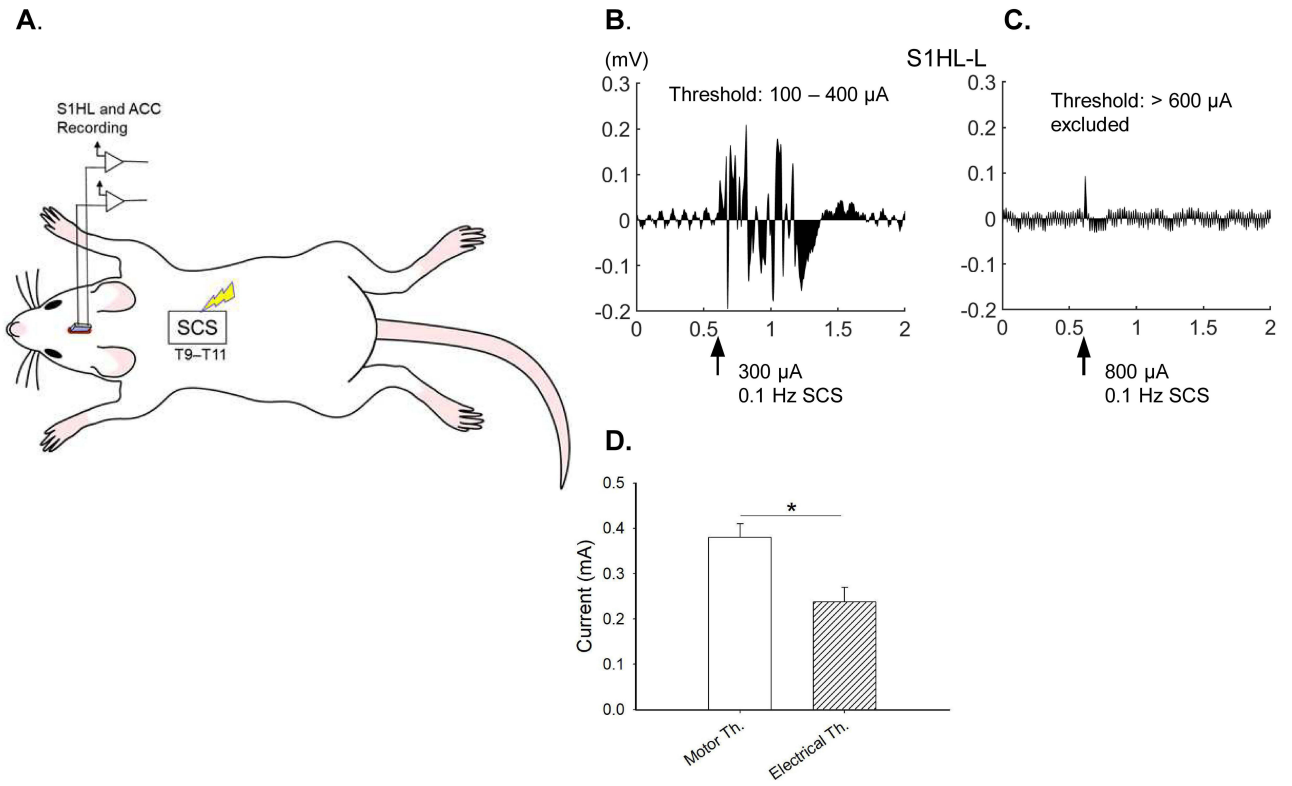

Figure 6 Impedance test to measure the thresholds of cortical evoked local field potentials (eLFP) and motor threshold (MoT) induced by SCS discharge. (**A**) Cartoon picture illustrates the discharge and recording; (**B**) An example of eLFP recording by slowly increasing SCS current amplitude to 300 μA (0.1 Hz, 1 ms, biphasic waves), indicating an intact electrode contact. (**C**) In case of inadequate eLFP recording when discharge as high as 800 μA, indicating electrode dysfunction or high impedance, rats were excluded from subsequent experiments. (**D**) Summaries of the Amplitudes of muscle threshold (Motor Th.) and cortical eLFP thresholds (Electrical Th.) induced by SCS. N = 5; * $p < 0.05$; Student's *t*-test.

significantly at the contralateral hind paw or in the control rats (Figure 7B). The PWTs of the sham surgery group remained unchanged after pUHF-SCS (Figure 7A, gray line). In contrast, pUHF-SCS significantly reversed the reduction in PWTs of the ipsilateral paw (Figures 7A, blue line) but had no effect at the SNI contralateral paw (Figures 7B, blue line). The inhibitory effect manifested one hour after pUHF-SCS, remained high for at least five hours, and then gradually decreased on the next day (Figures 7A). Strikingly, significant pain-suppressing effect after each pUHF-SCS persisted for two days (Figures 7A, blue line) and did not show tolerance after repeated treatments. In addition, our previous study demonstrated that pUHF-SCS could suppress SNI-activated C-component at the S1HL and ACC.[3]

SCS Electrodes Showed Increasing Impedance but Stabilized on Day 12 Post-Implantation

After implantation of the SCS device, a thin transparent fibrotic membrane developed between the inferior surface of the electrode and the spinal dural surface (Figure 8A), which could possibly cause current impedance. We measured the electrical impedances of distinct high-frequency at 10 kHz and 100 kHz with a U1733C LCR Meter (Keysight Technologies, Santa Rosa, CA, USA) and pUHF-SCS at 500 kHz with a Cube 2032 (Gimer Medical Co., New Taipei City, Taiwan). The impedances were similarly increased on post-implantation day 7 and reached a stable level after 12 days (Figure 8B). We speculate that the impedance increases due to the formation of the fibrotic membrane. We also observed a negative correlation between impedance increase and frequencies, which is consistent with previous studies.[13,14]

https://doi.org/10.2147/JPR.S489420

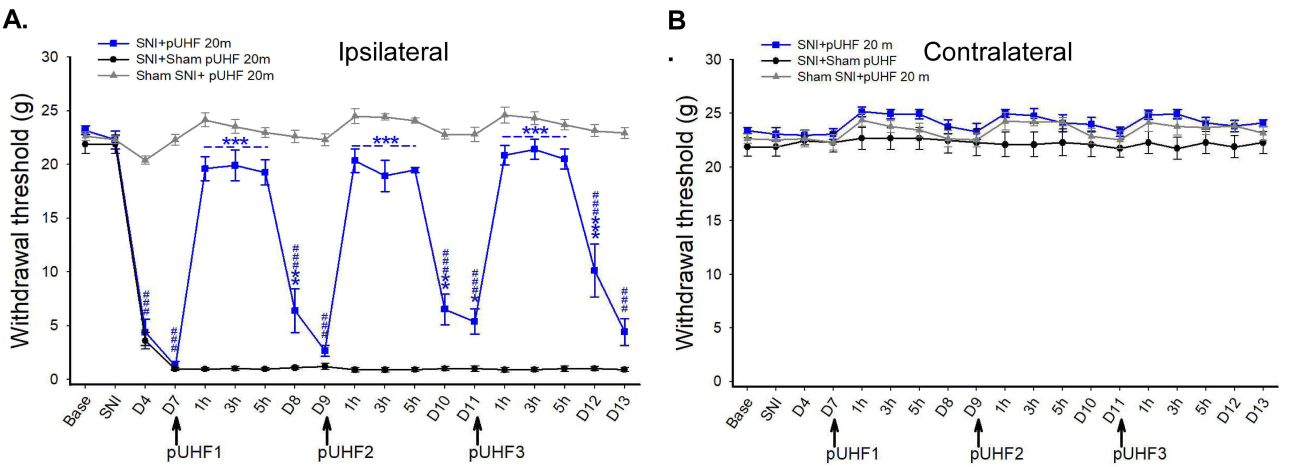

Figure 7 Comparisons of paw withdrawal thresholds (PWTs) following repeated 20-min pulsed ultrahigh-frequency SCS (pUHF-SCS) between the spared nerve injury (SNI) and the sham-operated rats. (**A**) PWTs of the ipsilateral hind paw after 3 sessions of pUHF-SCS among the SNI+pUHF 20m (n = 6), the SNI+Sham pUHF (n = 4) and the Sham SNI+pUHF (n = 7) groups. (**B**) No differences among groups at the contralateral hind paw. ### P < 0.001 vs Pre-SNI; ** P < 0.01, *** P < 0.001 indicate SNI+pUHF 20m vs SNI+ Sham pUHF 20m; two-way RM-ANOVA followed by Tukey post-hoc test.

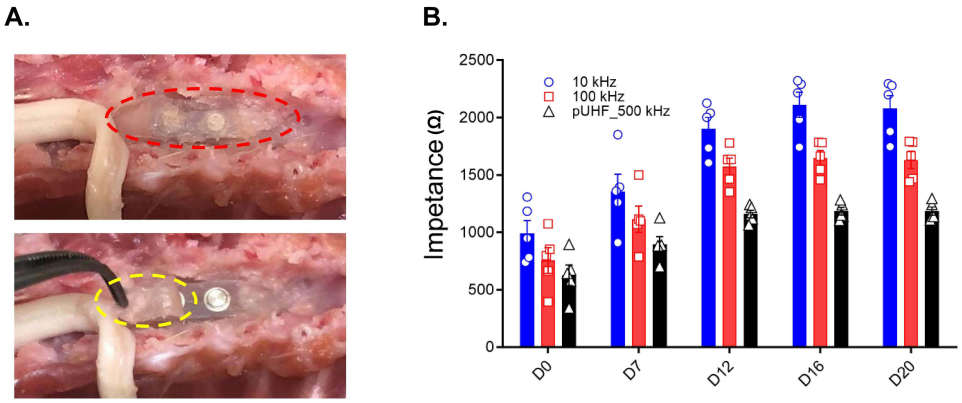

Figure 8 Comparisons of the electrode impedance among different high-frequency SCSs. (**A**). Anterior-posterior views of the spinal cord and bipolar electrode. In the upper panel, the red dashed oval highlights a thin, transparent fibrotic membrane that has formed between the spinal cord and the electrode. In the lower panel, the yellow dashed oval marks a partially opened fibrotic membrane, exposing the SCS electrode. (**B**). The impedance of three high-frequencies SCS (10K, 100K, and 500kHz) at different time points. Impedance values increased over time and stabilized after 12 days post-implantation. No significant differences between 12, 16, and 20 days for each frequency. N = 5; p > 0.5; one-way repeated measures ANOVA followed by Tukey *post-hoc* test.

Electrode Implantation Did Not Change the Cortical eLFPs

We conducted experiments with more sophisticated stimulation tests to demonstrate the safety of implanting SCS electrodes as a supplement. The AUCs of the eLFPs in bilateral S1HL and ACCs did not change between before SCS implantation and 7 days afterward, but stepwise increased when stimulation intensities from 0 (baseline), 0.5 mA (low), 1 mA (medium), to 5 mA (high) at the hind paw in naive rats (Figure 9). Furthermore, the rats showed preserved normal motor functions and no observable behavioral abnormalities, further supporting the safety of prolonged epidural implantation of SCS electrodes in this model.

Discussion

The study was an extension of our previous article in *Anesthesiology* to present more details on the methodology.[3] We delineated the methodology for establishing a stable rat model featuring epidural SCS and electrophysiological recordings of cortical eLFPs elicited by hind paw electrical stimulation. The position and method of needle electrodes inserted at the hind paw for stable and distinguishable cortical eLFPs were carefully defined. SNI-enhanced C components at brain were responsive to electrical stimulation majorly at the contralateral but not the ipsilateral hind paw. We developed

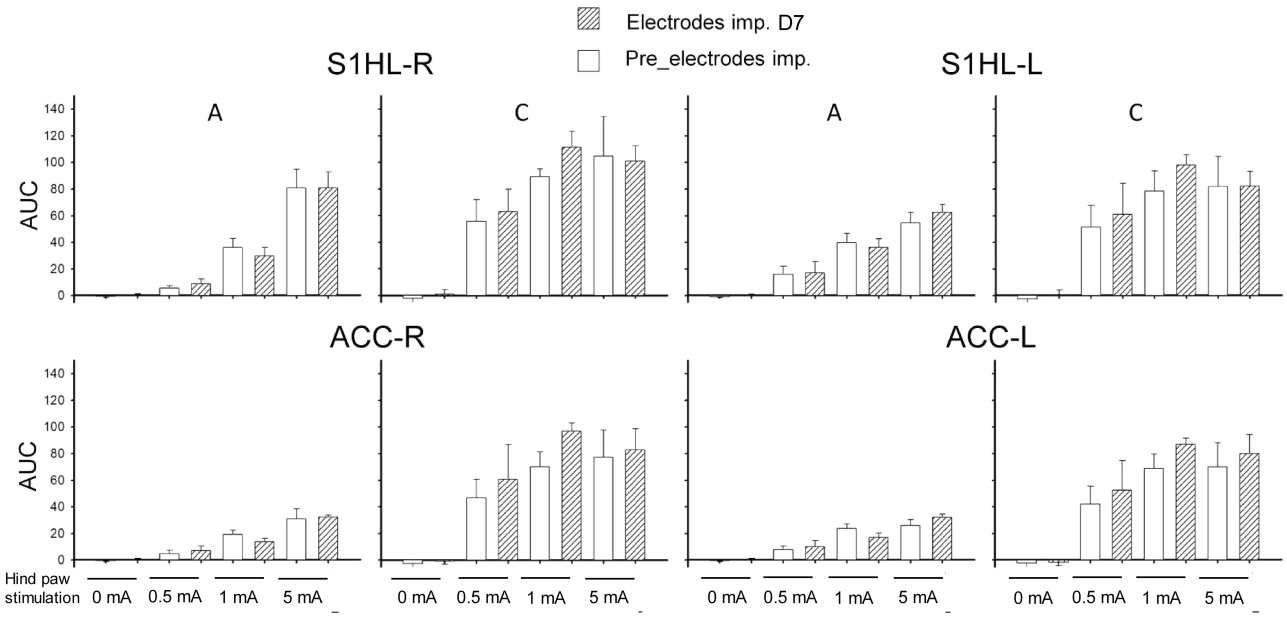

Figure 9 The implantation of SCS electrodes did not alter the cortical evoked local field potentials (eLFPs) in naive rats. The eLFPs were elicited by 0 (baseline), low (0.5 mA), medium (1 mA), and high intensity (5 mA) electrical stimulation at the hind paw before electrode implantation and on Day 7 after implantation. The area under the curves (AUCs) of eLFPs recorded at the bilateral primary somatosensory cortex of the hind limb (S1HL) and anterior cingulate cortex (ACC) showed no differences before and after electrode implantation. N = 6; Paired *t*-test.

an impedance test to confirm the optimal SCS electrode contact with the spinal dura by identifying the threshold to activate cortical eLFPs and the MoT of hind limbs. We also found the growth of a fibrotic membrane beneath SCS electrode, which may increase the electrical impedance. Finally, we could demonstrate the effectiveness of a newly developed pUHF-SCS paradigm in this model.

The brain mechanisms underlying the effects of SCS remain elusive due to a lack of consensus animal models. This study established an in vivo electrophysiological brain recording platform for exploring alterations in the rat brain. The cortical eLFPs at the S1 and ACC could be analyzed over time, under various noxious conditions, and with any SCS parameters. One intriguing pitfall in the SNI model was the electrical stimulation side at the paw. Central sensitization, a process that amplifies pain relativities within the central nervous system, has long been recognized in the development of neuropathic pain following peripheral nerve injury.[15] SNI can lead to central sensitization,[16,17] as evidenced by an enhancement of the C components of eLFPs elicited by stimulation of the contralateral hind paw after SNI. In SNI surgery, the tibial and common peroneal nerves were transected, preserving the sural nerve. After SNI, the remaining sural nerve in the injured hind limb exhibited structural plasticity, especially Nav1.8-positive nociceptors would reorganize and re-territorialize to the denervated areas.[18] This structural plasticity process is slow and progressively changed, which may result in complex nociceptive responses to stimulation of the injured paw, with considerable variability among individual rats. Consequently, we did not observe an enhancement of eLFPs in response to stimulation of the ipsilateral hind paw at seven days after SNI. Although much remains unknown about the SNI-induced structural plasticity of c-fibers, a similar finding had been reported that von-Frey noxious stimulation of the contralateral (uninjured) paw elicited greater evoked calcium neuronal activity in the ACC of mice with SNI compared to stimulation of the ipsilateral (injured) paw.[19] In complete Freund's adjuvant injection-induced inflammatory pain models and SNI-induced neuropathic pain models, stimulation of the hind paw contralateral to the injured side augmented brain potentials at the ACC and S1.[20–22] However, future studies that prioritize influences of the brain's sensitization in response to hind-paw ipsilateral noxious stimulation are still necessary.

Producing consistent and faithful eLFPs in the brain is also essential. Electrical stimulation at the sural nerve-innervated area, ie, the lateral border of the hind paw between the hairy and glabrous skin over the fifth toe, elicits stronger brain activities than stimulation at the tibial nerve-innervated territory on day seven post-SNI. This location,

https://doi.org/10.2147/JPR.S489420

predominantly innervated by spared sural nerve fibers,[23,24] exhibits a high density of Aδ- and C-nociceptors[25] and is an acceptable site for neurophysiological studies.

While electrodes are ideally positioned on the dorsal dura during surgery, there remains a risk of electrode migration, deviation, and other complications, such as spinal cord damage, vascular compression, infection, or hemorrhage. An anchor was sutured onto the muscle for firm fixation to avoid migration. To early detect electrode dislodgement and confirm its function, we designated an impedance test by setting 100–400 μA as a threshold range of SCS discharge (PW = 1 ms, 0.1 Hz, biphase) to activate cortical eLFPS and 150–600 μA as threshold to activate MoT at the hind limb (Figure 6). We found that the rats qualifying these criteria demonstrated prolonged and effective analgesia induced by 20-min pUHF-SCS, affirming the feasibility of this SCS impedance test.

The time-dependent increase in electrode impedance, presumably due to the growth of a fibrotic membrane between the electrode and the dura, could reach stable and then be unchanged after day 12 post-implantation (Figure 8B for days 12, 16 and 20). In addition, since higher frequency SCS had lower impedance compared at the same time point (ie, impedance: pUHF [500 kHz] < 100 kHz < 10 kHz), it may be assumed that higher frequency SCS has a better chance to produce stronger effectiveness by lower delivery energy or "charge per second".[26,27] We are validating this assumption by using this rat model.

In this study, major surgeries and device implantations were performed, each carrying potential risks and complications. Our previous study[3] reported that Luxol Fast Blue (LFB) staining and Hematoxylin-Eosin (H&E) staining showed no marked morphological deformity in the spinal cord between the naïve rats and those treated with 20-minute pUHF-SCS. Furthermore, our previous study indicated that long-term SCS implantation and repeated pUHF-SCS (~28 days) did not cause immediate or delayed behavioral abnormalities, such as standing still, limping, cramping, or walking difficulties, or changes in the Rotarod motor tests. In addition, there was no evidence of increases in immune-cell infiltration, sensitized neuron or glial cells, demyelination, or cleaved caspase 3-positive apoptotic neurons by immunostaining.[3] In this study, we further demonstrated that implantation of the SCS electrodes did not alter the cortical eLFPs at bilateral brain areas, suggesting full preservation of orthodromic transmission in this model. These findings suggest that spinal electrode implantation and pUHF-SCS did not cause spinal cord damage by the end of this study. Given the chronicity of neuropathic pain and the year-long application of SCS in humans, much longer implantation time and long-term SCS treatment for over months are required to validate the safety and applicability of this platform.

Conclusions

We detailed the methodology and pitfalls for establishing a reliable and stable rat model featuring epidural SCS and recordings of cortical eLFPs elicited by hind paw electrical stimulation. This study supports our previous findings that the pUHF-SCS can effectively induce analgesic effects on neuropathic pain in rat models and this platform can serve as an experimental tool for comparing effects and underlying MoA among various SCS modalities, such as LF-SCS, HF-SCS, burst SCS and pUHF-SCS. We believe such a rat model can become a commonly used tool for medical translation and mechanism-based analysis of SCS.

Ethics Approval

All experimental procedures adhered to the guidelines set by the Academia Sinica Institutional Animal Care and Utilization Committee, Taipei, Taiwan. The experimental protocol was approved by the Institutional Animal Care and Use Committee (IACUC) (Protocol No.: 23-06-2018).

Author Contributions

All authors made a significant contribution to the work reported, whether that is in the conception, study design, execution, acquisition of data, analysis and interpretation, or in all these areas; took part in drafting, revising or critically reviewing the article; gave final approval of the version to be published; have agreed on the journal to which the article has been submitted; and agree to be accountable for all aspects of the work.

Funding

This study was supported by the Institute of Biomedical Sciences at Academia Sinica (grant numbers IBMS-CRC111-P02 [to Y.R.W. and C.C.C.]) and Academia Sinica (grant numbers AS-IA111-L06 [to C.C.C.]).

Disclosure

Yeong-Ray Wen is a scientific consultant and stockholder of Gimer Medical Co.; Wei-Tso Lin is the Chief Executive Officer of Gimer Medical Co.; Kuo-Hsiang Lu is a preclinical specialist at Gimer Medical Co. The company did not provide financial support for this paper. The authors report no other conflicts of interest in this work.

References

1. Cohen SP, Mao J. Neuropathic pain: mechanisms and their clinical implications. *BMJ*. 2014;348. doi:10.1136/bmj.f7656
2. Joosten EA, Franken G. Spinal cord stimulation in chronic neuropathic pain: mechanisms of action, new locations, new paradigms. *Pain*. 2020;161 Suppl 1(1):S104–S113. doi:10.1097/j.pain.0000000000001854
3. Yang CT, Guan Y, Chen CC, et al. Novel pulsed ultrahigh-frequency spinal cord stimulation inhibits mechanical hypersensitivity and brain neuronal activity in rats after nerve injury. *Anesthesiology*. 2023;139(5):646–663. doi:10.1097/ALN.0000000000004680
4. Lee SY, Hsiung NH, Chapman KB, et al. A pilot study of novel ultrahigh-frequency dorsal root ganglia stimulation for chronic lower limb pain: focusing on safety and feasibility. *Pain Pract*. 2024;25(1). doi:10.1111/papr.13436
5. Reinders LJ, Luijten JA, Frankema SP, Huygen FJ, de Vos CC. The effect of various spinal neurostimulation paradigms on the supraspinal somatosensory evoked response: a systematic review. *Neuromodulation*. 2024;27(6):1008–1019. doi:10.1016/j.neurom.2024.04.003
6. Heijmans L, Zhang TC, Esteller R, Joosten EA. Ninety-Hz spinal cord stimulation-induced analgesia is dependent on active charge balance and is nonlinearly related to amplitude: a sham-controlled behavioral study in a rodent model of chronic neuropathic pain. *Neuromodulation*. 2024;27 (1):95–107. doi:10.1016/j.neurom.2023.09.005
7. Shu B, He SQ, Guan Y. Spinal cord stimulation enhances microglial activation in the spinal cord of nerve-injured rats. *Neurosci Bull*. 2020;36 (12):1441–1453. doi:10.1007/s12264-020-00568-6
8. Vallejo R, Kelley CA, Gupta A, Smith WJ, Vallejo A, Cedeno DL. Modulation of neuroglial interactions using differential target multiplexed spinal cord stimulation in an animal model of neuropathic pain. *Mol Pain*. 2020;16:1744806920918057. doi:10.1177/1744806920918057
9. Xiao Z, Martinez E, Kulkarni PM, et al. Cortical pain processing in the rat anterior cingulate cortex and primary somatosensory cortex. *Front Cell Neurosci*. 2019;13:165. doi:10.3389/fncel.2019.00165
10. Chaplan SR, Bach FW, Pogrel JW, Chung JM, Yaksh TL. Quantitative assessment of tactile allodynia in the rat paw. *J Neurosci Methods*. 1994;53 (1):55–63. doi:10.1016/0165-0270(94)90144-9
11. Huang RY, Poree L, Ho KY, et al. Behavioral survey of effects of pulsed radiofrequency on neuropathic and nociceptive pain in rats: treatment profile and device implantation. *Neuromodulation*. 2020;24(8):1458–1466. doi:10.1111/ner.13169
12. Huang RY, Liao CC, Tsai SY, et al. Rapid and delayed effects of pulsed radiofrequency on neuropathic pain: electrophysiological, molecular, and behavioral evidence supporting long-term depression. *Pain Physician*. 2017;20(2):E269–E283.
13. Lorenzo MF, Bhonsle SP, Arena CB, Davalos RV. Rapid impedance spectroscopy for monitoring tissue impedance, temperature, and treatment outcome during electroporation-based therapies. *IEEE Trans Biomed Eng*. 2021;68(5):1536–1546. doi:10.1109/TBME.2020.3036535
14. Prakash S, Karnes MP, Sequin EK, et al. Ex vivo electrical impedance measurements on excised hepatic tissue from human patients with metastatic colorectal cancer. *Physiol Meas*. 2015;36(2):315–328. doi:10.1088/0967-3334/36/2/315
15. Shepherd AJ, Mickle AD, Golden JP, et al. Macrophage angiotensin II type 2 receptor triggers neuropathic pain. *Proc Natl Acad Sci U S A*. 2018;115(34):E8057–E8066. doi:10.1073/pnas.1721815115
16. Smith AK, O'Hara CL, Stucky CL. Mechanical sensitization of cutaneous sensory fibers in the spared nerve injury mouse model. *Molecular Pain*. 2013;9:1744–8069–9–61. doi:10.1186/1744-8069-9-61
17. Hu X, Du L, Liu S, et al. A TRPV4-dependent neuroimmune axis in the spinal cord promotes neuropathic pain. *J Clin Invest*. 2023;133(5). doi:10.1172/JCI161507
18. Hameed S. Na(v)1.7 and Na(v)1.8: role in the pathophysiology of pain. *Mol Pain*. 2019;15:1744806919858801. doi:10.1177/1744806919858801
19. Zhao R, Zhou H, Huang L, et al. Neuropathic pain causes pyramidal neuronal hyperactivity in the anterior cingulate cortex. *Front Cell Neurosci*. 2018;12:107. doi:10.3389/fncel.2018.00107
20. Friesner ID, Martinez E, Zhou H, et al. Ketamine normalizes high-gamma power in the anterior cingulate cortex in a rat chronic pain model. *Mol Brain*. 2020;13(1):129. doi:10.1186/s13041-020-00670-w
21. Zhang Q, Xiao Z, Huang C, et al. Local field potential decoding of the onset and intensity of acute pain in rats. *Sci Rep*. 2018;8(1):8299. doi:10.1038/s41598-018-26527-w
22. Shinoda M, Fujita S, Sugawara S, et al. Suppression of superficial microglial activation by spinal cord stimulation attenuates neuropathic pain following sciatic nerve injury in rats. *Int J Mol Sci*. 2020;21(7):2390. doi:10.3390/ijms21072390
23. Decosterd I, Woolf CJ. Spared nerve injury: an animal model of persistent peripheral neuropathic pain. *Pain*. 2000;87(2):149–158. doi:10.1016/S0304-3959(00)00276-1
24. Kambiz S, Baas M, Duraku LS, et al. Innervation mapping of the hind paw of the rat using Evans Blue extravasation, Optical Surface Mapping and CASAM. *J Neurosci Methods*. 2014;229:15–27. doi:10.1016/j.jneumeth.2014.03.015
25. Leem JW, Willis WD, Chung JM. Cutaneous sensory receptors in the rat foot. *J Neurophysiol*. 1993;69(5):1684–1699. doi:10.1152/jn.1993.69.5.1684
26. Miller JP, Eldabe S, Buchser E, Johanek LM, Guan Y, Linderoth B. Parameters of spinal cord stimulation and their role in electrical charge delivery: a review. *Neuromodulation*. 2016;19(4):373–384. doi:10.1111/ner.12438
27. Chen Z, Huang Q, Yang F, et al. The impact of electrical charge delivery on inhibition of mechanical hypersensitivity in nerve-injured rats by sub-sensory threshold spinal cord stimulation. *Neuromodulation*. 2019;22(2):163–171. doi:10.1111/ner.12910